Snow Engineering, Hjorth-Hansen, Holand, Løset & Norem (eds) © 2000 Balkema, Rotterdam, ISBN 90 5809 148 1

The snowdrift pattern around two cubical obstacles with varying distance – Measurements and numerical simulations

Thomas K.Thiis
Narvik Institute of Technology, The University Courses on Svalbard, Norway
Christian Jaedicke
The University Courses on Svalbard, Norway

ABSTRACT: Snowdrifts around buildings can cause serious problems when formed on undesirable places. The formation of snowdrifts is highly connected to the wind pattern around the building, and the wind pattern is again dependent on the building design and the position of the surrounding buildings. The snowdrift pattern around two 2.5m cubes, positioned close to perpendicular to the wind direction is investigated. The spacing between the cubes was varied to investigate the effects of a local wind speedup between the cubes. The measurements show that a large snowdrift forms between the cubes with the largest spacing between them. A smaller spacing between the cubes results in the disappearance of the centre snowdrift. The reason for this is that the small spacing causes the formation of one horse shoe vortex encirceling both cubes and decreasing the amount of snow entering the zone between the cubes. The wind speedup between the cubes will also sweep the area clean of snow. The upwind wind direction, the vertical wind speed profile and the blowing snow flux is measured during the experiments. The experiments were conducted in a valley 3 km wide and 20 km long on Spitsbergen, Norway. The wind in this valley is blowing in the same direction approximately 90% of the time during winter and the site is well suited for studies of snowdrifts and snowdrifting. The different experiment configurations are investigated through numerical simulations, which confirms the measurements. The numerical method can be applied to other building configurations of limited complexity to determine the optimum position of buildings in clusters.

1 INTRODUCTION

The design of buildings in windy and snowy areas requires consideration of the wind transported snow and the snowdrifts formed thereof. The topic of snowdrift formation has previously been studied by the means of full scale experiments, wind tunnel simulations and numerical analysis. Full scale measurements is sparsely reported, however, Haehnel and Lever (1994) have compiled field data from several sources and assessed the properties regarding model validation. Thiis and Gjessing (1999) studied the position and relative size of snowdrifts around cubical obstacles with different rooftops and emphasised on the snowdrifts formed upwind and at the sides of the obstacles.

Numerical analysis of snowdrifts around buildings has been performed by i.a. Tominaga and Mochida (1999), Thiis (2000), Bang et. al. (1994), Kawakami et. al. (1997), Uematsu et.al. (1991). Common for these studies is that the wind field is determined by solving the time averaged Navier-Stokes equations and the blowing snow is then coupled to the wind field. The differences lays mainly in the applied turbulence model and the coupling of the snow phase. A widely used turbulence model is the k-ε model. Even if this model is known to calculate too high turbulence intensity near impinging surfaces and reattachment zones, it produces realistic wind patterns around buildings.

Snow can be transported in three different modes; creep, saltation and suspension. The creep mode is because of its limited transported snow quantity, usually neglected when considering mass transport. Saltating particles follows jumping particle paths in the lower tens of centimetres near the surface. Suspension transport mode is initiated when the saltating snow particles are picked up by the wind and transported in the boundary layer without contact with the surface.

A key property of the snow cover when considering blowing snow is the snow threshold friction velocity, u_{*_t}. This is the friction velocity of the wind when particle ejection from the surface cease, and it is ranging from 0.07 to 0.25 m/s for fresh, dry snow and from 0.25 to 1 m/s for old, wind hardened snow (Kind, 1981). Assuming that the vertical wind profile follows the widely used logarithmic expression, the friction velocity of the wind, u_*, can be found from

$$u_* = u(z)\kappa / \ln\left(\frac{z}{z_0}\right) \qquad (1)$$

where $u(z)$ is the wind speed in height z, κ is the von karman constant and z_0 is the roughness, deduced from wind speed measurements in two heights, and the expression

The wind pattern around a cube is described by Castro and Robins (1977) and Martinuzzi and Tropea (1993). They describe a recirculation zone up-

$$z_0 = \exp\left(\frac{u(z_2)\cdot\ln(z_1) - u(z_1)\cdot\ln(z_2)}{u(z_2) - u(z_1)}\right) \qquad (2)$$

wind the cube forming between the stagnation point on the upwind wall and the surface. This recirculation zone is extending upwind to the upwind stagnation point and is deflected downwind the sides of the cube, creating a horseshoe shaped system of vor-

$$R = 1.6\sqrt{ah} \qquad (3)$$

tices. Downwind the cube, between the horseshoe vortices, there is a wake region extending downwind to the downwind reattachment point. Beranek (1984) suggested two rules for the determination of the influence area around buildings of rectangular shape. A circle with the radius

can be drawn trough the front and rear stagnation points. The distance from the centre of the circle , M, to the windward face of the building is then found from

$$e = 0.9\sqrt{ah} \qquad (4)$$

here h and a is respectively the height and width of the windward wall. The expressions are based on flow visualisation in wind tunnel experiments, and are valid for $1.22 > h/a > 0.33$ and certain upwind wind and turbulence intensity profiles. It is said that buildings with no overlap of their influence area will not interact. For cubical obstacles this means a distance of $d = 2.5h$. Beranek also suggests that if the distance between the buildings is small, the two buildings begin to act as one building with a long windward wall. They develop a common horseshoe shaped vortex system encirceling both buildings, and not separate systems of vortices between the buildings.

It has been observed that a large centre snowdrift is forming between buildings with a spacing between them. However, if the spacing is under a certain limit, this snow drift does not form. It is believed that due to the funnel shape of the passage between the buildings, the wind speed is increased and is sweeping the passage free from snow.

The phenomenon of centre snowdrift between buildings is in this report studied in detail by the means of field experiments and numerical analysis.

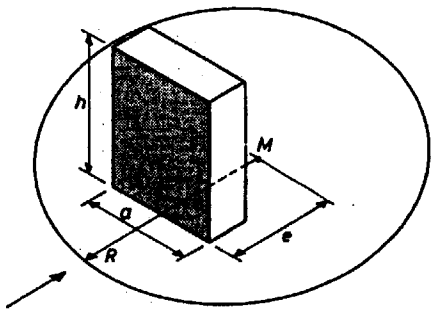

Figure 1. Influence area around buildings of rectangular shape (Beranek, 1984)

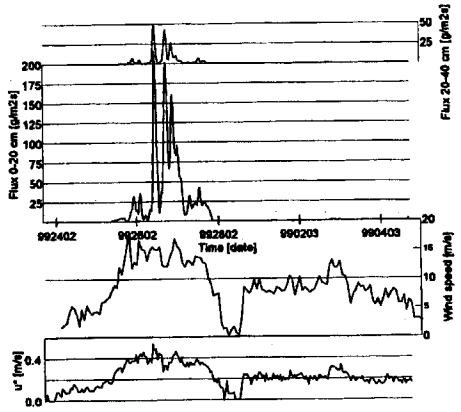

Figure 2. Wind speed in 10m height, friction velocity and snow drifting flux in heights 0-20cm and 20-40 cm during case A

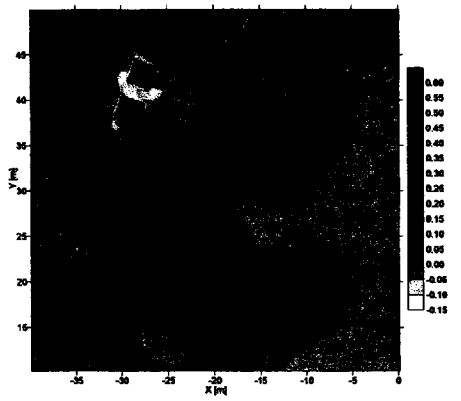

Figure 3. Contour map of snowdrift pattern, and main wind direction in case A

Table 1 Overview of the experiment setup

	Case A	Case B	Case C
Time	10 days	11 days	14 days
Distance btw. cubes	1.7m	4.8m	5.9m

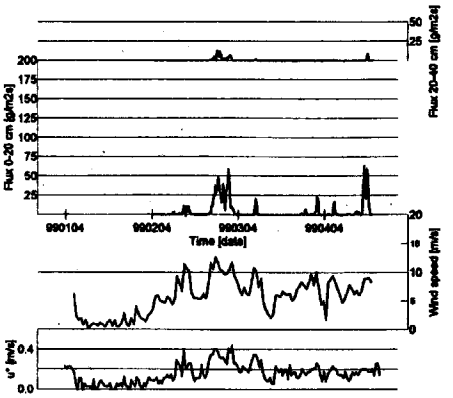

Figure 4. Wind speed in 10m height, friction velocity and snow drifting flux in heights 0-20 cm and 20-40 cm during case B

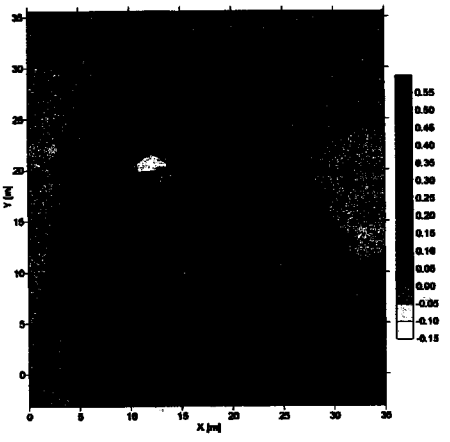

Figure 5. Contour map of snowdrift pattern, and main wind direction around case B

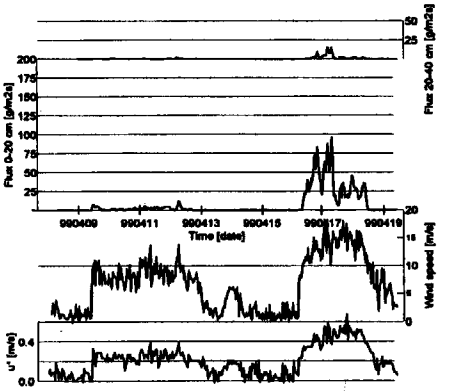

Figure 6. Wind speed in 10m height, friction velocity and snow drifting flux in heights 0-20 cm and 20-40 cm during case C

Since the deposition of the centre snowdrift is, among other factors, dependent upon the wind speed between the buildings, it is evident that the incidence angle of the wind has influence on the formation of the centre snowdrift. In the field experiments of this study, there is a variation of the incidence angle of the wind which makes it difficult to make exact comparisons to Beraneks work, however, the main features of the flow remain.

2 FIELD SETUP

The winter of 1999 a series of experiments were performed in Adventdalen on the arctic island Spitsbergen, Norway. Three of the experiments considered the formation of the centre snowdrift forming between two buildings with varying distance. Two 2.5m cubical shaped obstacles were placed on the flat, uniform surface of a wide valley. The wind pattern in this valley has previously been found to be mainly down the valley during winter. The yearly precipitation in the valley is very low and the thickness of the snow cover was approximately 200 mm of hard wind packed snow. The small amount of precipitation combined with the uniform wind direction makes the area well suited for snowdrift experiments because accumulated, wind transported snow show a very distinct pattern compared to areas with more precipitation. The incidence angle of the wind on the cubes in the tree different experiments was varying from 15 to 26 deg.

After some days of snowdrifting, significant snowdrifts were developed around the cubes, and the experiment was moved upwind to avoid disturbance from the previous experiment. The distance between the cubes was altered, and a new snowdrift was developed. This was repeated again with a new spacing. An overview of the experiments is presented in table 1. After each experiment, the snowdrift's size and shape were measured with a surveying total station. The Kriging method was used to interpolate a surface between the measured points. The deposited snow was very compact with a surface of high hardness.

The upwind wind profile and direction was measured in four heights up to 10m on an automatic weather station. The wind speed sensors were of the cup anemometer type and the sampling interval was ten minutes. The presented plots shows the 1 hour average of the wind speed measurements. The upwind snow drifting flux was measured in two averaged levels, 0-20cm and 20-40cm above the surface. The instrument in use was the FlowCapt sensor from IAV Engineering (Chritin et.al., 1999). The sampling interval was 15 seconds with the 1 hour averaged values presented in the plots. The detection principle of this sensor is based on a mechanical-acoustical coupling. It consists of closed tubes con-

taining electro-acoustical transducers. The signal from the transducers is filtered and a signal proportional to the particle flux is produced.

2.1 *Case A*

Wind speed, friction velocity and snow drifting flux during case A is shown in figure 2. The main snow flux occurred between 25. and 28. february. It can be seen from the friction velocity plot and the lower snow drifting flux plot that the threshold friction velocity is approximately 0.20 m/s.

Figure 3 shows the snow drift pattern around the two 2.5m cubes in case A. The distance between the cubes was 1.7m and incidence angle was approximately 26°. The upwind snowdrift is continuos transverse of the wind direction, with no local minimum height. This, together with the fact that the centre snowdrift is missing, indicates that there is only one horse shoe vortex, encirceling the two cubes. The maximum distance between the upwind snowdrift and the cubes is found on the most upwind cube and is approximately 1.6m, measured perpendicular to the upwind wall. The distance between the upwind snowdrift and the other cube is approximately 1.35m. Just downwind of the cubes, two leeward snowdrifts have developed. The development rate of the leeward snowdrifts seems to be much smaller than the snowdrifts upwind and on the sides of the building. This is probably because the flux of snow into the wake area is low compared to the surrounding area of the building. The snow is ploughed to the sides and prevented from entering the low surface shear stress area downwind of the cubes.

2.2 *Case B*

Wind and snow drifting flux data during case B is shown in figure 4. Just ahead of the experiment there was a small snowfall making the threshold friction velocity for snow drifting slightly lower than in case A, approximately 0.18 m/s. The main snow transport occurred between the 2. and the 3. of april. The resulting snowdrift pattern from case B is shown in figure 5. The distance between the cubes was 4.8m and the incidence angle of the wind was approximately 16°. Here, there is a tendency for deposition of a centre snowdrift. The upwind snowdrift have two local maximum heights just in front of each cube, indicating the presence of two horse shoe vortices. However, there is no snow deposition just between the cubes, the centre snowdrift starts just downwind the cubes and extends parallel to the lateral snowdrifts. The centre snowdrift is slightly higher than the lateral snowdrifts, but the downwind extension is smaller than for the two lateral snowdrifts. The distance between the upwind snowdrift and most upwind cube is approximately the same as for the case A, 1.6m and slightly less for the other cube.

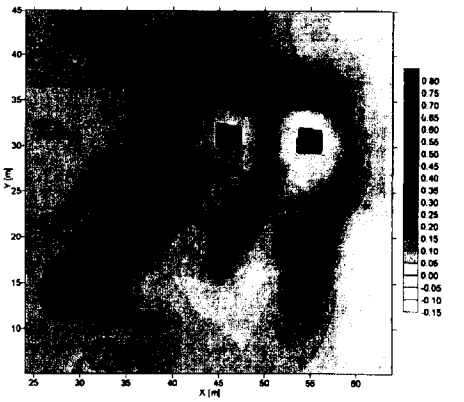

Figure 7. Contour map of snowdrift pattern and main wind direction in case C

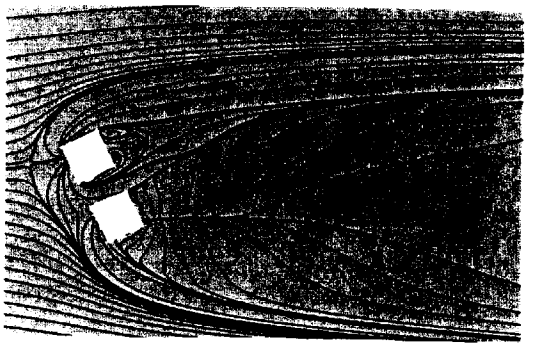

Figure 8. Streamlines around case A near the surface.

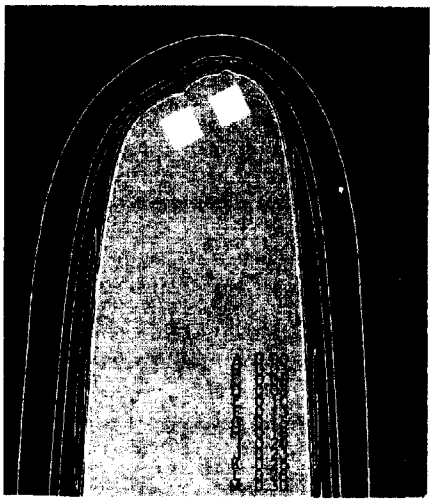

Figure 9. Contoured map of the fluid density 1.41kg/m^3, case A.

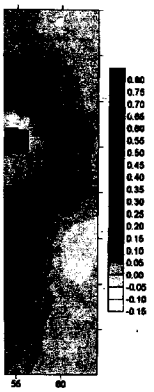

pattern and main wind

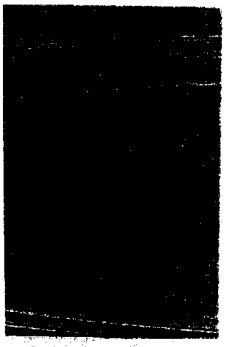

near the surface.

l density 1.41kg/m^3, case

2.3 *Case C*

Wind and snow drift flux data during case C is shown in figure 6. It can be seen that the snowdrifting occurred in two episodes, 9-13.apr. and 16-18.apr. the threshold friction velocity was approximately 0.20 m/s for the first episode, and slightly larger for the second episode. The snowdrift pattern around case C is shown in figure 7. Here a distinct centre snowdrift developed during the first wind episode, and which was enlarged during the second episode. The height of the centre snowdrift was 0.80m which is considerably larger than for the two lateral snowdrifts. The presence of two horseshoe vortices is evident in that the snowdrift pattern looks similar to the ones forming around two single cubes with the two adjacent lateral snowdrifts joining together in one large centre snowdrift. The centre snowdrift does, however, not reach as far downwind as any of the lateral snowdrifts. The distance between the cubes was 5.9m and the incidence angle of the wind was 17°. The distance between the cubes and the upwind snowdrift was approximately 1.6m.

3 NUMERICAL SIMULATIONS:

To simulate the wind field and snow drifting around the cubes, a general purpose finite volume CFD code was applied. The CFD code solves the incompressible, time averaged Navier-Stokes equations, using a k-ε turbulence model to close the equations. The turbulence model is known to compute excessive turbulence near the edges of the windward walls, which also can affect the downwind wakes. It is however widely used, and it is capable to produce realistic wind patterns around buildings.

The computational domain is 85x60x15m and consists of 90x89x23 grid cells with grid refinement near the obstacles. The inlet vertical wind velocity profile to the computational domain follows the logarithmic expression from equation 1. The roughness height z_0 is set to 0.002m, which is equal to the upwind measurements, κ is set to 0.4 and u_* is equal to 0.6 m/s. This corresponds to a wind velocity of approximately 12 m/s at a 10 m height. The turbulence intensity on the inlet boundary is set to 0.05. This conserves the vertical wind profile through the computational area which is not affected by the cube. The outlet boundary is continuative, meaning that the normal derivatives of all quantities are set to zero. On the surface boundaries, a law-of-the wall velocity profile is assumed. The lateral and top boundaries have symmetry conditions.

The movement of the snow phase relative to the wind is found using the drift-flux approximation (Thiis, 2000; Flow Science, 1997; Bang et.al., 1994)

$$u_r = D_f f_1 f_2 \left(\frac{\rho_2 - \rho_1}{\rho_1} \right) \frac{1}{\rho} \nabla p \qquad (5)$$

Here ∇p is the pressure gradient, f is volume fraction, ρ is density and the subscripts *1* and *2* denotes the two different fluids. The total mixture density is $\rho = f_1\rho_1 + f_2\rho_2$. D_f is a coefficient related to the friction between the snow phase and the air, found by balancing the drag force on a sphere with the buoyancy force.

$$D_f = \frac{2r_0^2}{9\nu} \qquad (6)$$

Here r_0 is the mean radius of the snow particles and ν is the kinematic viscosity of the air.

Other properties used in the simulations are the density and the dynamic viscosity of air at –20 °C which is set to 1.38 kg/m^3 and 1.63*10^{-5} N*s/m^2 respectively, the density of snow particles, set to 400 kg/m^3 and the apparent threshold viscosity of the snow phase. This property is defined to be

$$\mu_{app} = \rho_{air} u_{*_t}^2 \left(\frac{dz}{du} \right)_{surface} \qquad (7)$$

(Thiis, 2000) where u_{*_t} is set to 0.2 [m/s] and the vertical wind speed gradient is found using equation 1, substituting u_* with u_{*_t}. This results in an apparent viscosity of μ_{app}=2.2*10^{-4} N*s/m^2. The mixture viscosity in the computational cells is evaluated as a volume fraction weighted average of the two constant viscosities. The vertical blowing snow density profile on the inlet is equal to the measured profile of a situation with a 10m wind speed of 12 m/s.

The simulation model calculates the snowdrifting density around the buildings, increasing the viscosity were the snow density is high. A high viscosity slows down the air velocity and increases the density even more. Since the model does not create a new surface, the pattern showed is only the initial snow deposition area which is determined by the surface shear stress and the blowing snow density. It is assumed that the relative size of the snowdrifts can be suggested on this basis.

3.1 *Case A*

Figure 8 shows the streamlines around case A near the ground surface. It can be seen that the streamlines form only one horseshoe vortex encirceling both cubes. The vortex acts like a canopy and prevents snow from entering the space between the cubes.

This can also be seen on figure 9 where the simulated snowdrifting is shown. The snowdrifts are expressed as iso-surfaces of density. The height of the iso-surface is shown as a contoured map. The two lateral snowdrifts show increased height downwind of the cubes with slightly higher contours of the snowdrift near the most downwind cube. The positions of the downwind maximum heights are however not very accurately calculated and located too far downwind. The reason for this might be the tur-

bulence model calculating too much turbulence near the cubes, thus extending the wake area. The upwind snowdrift shows the same variation as the measured data with a slightly larger distance between the most upwind cube and the snowdrift than the neighbouring cube. Assuming that the edge of the upwind snowdrift is positioned at the upwind edge of the horseshoe vortex, the distances from the cubes to the snowdrift are 2.3m and 1.8m respectively.

3.2 *Case B*

The simulations of the wind pattern around case B is shown in figure 10.
The streamline visualisation show two separate sets of horseshoe vortices and corresponding wake areas. This corresponds to the assumption made on the basis of the presence of an observed centre snowdrift. The snowdrifting calculations on figure 11 also show increased snow density between the cubes. The position of this increased snow density area is between the cubes, where the measurements show no snow deposition at all. The measured centre snowdrift is positioned further downwind, and the area between the cubes might be submitted to erosion. However, the computed position of the two upwind snowdrifts show reasonable agreement with the measurements. The distances are 1.8m and 1.7m respectively, which is considerably better than for case A. The lateral snowdrifts are calculated too far downwind, again an effect of the extended wake caused by excessive turbulence generation near the upwind walls.

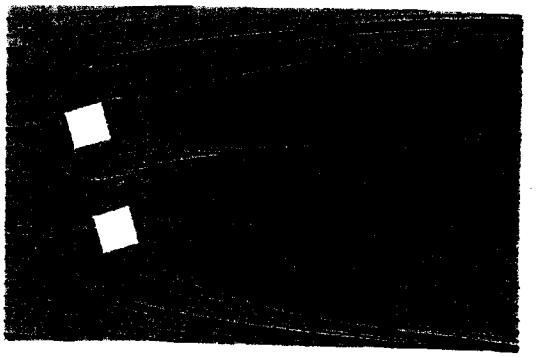

Figure 10. Streamlines around case B

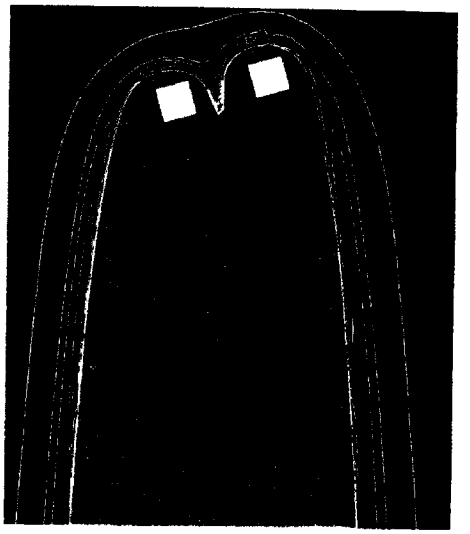

Figure 11. Contoured map of fluid density 1.41 kg/m^3 around case B

3.3 *Case C*

The streamlines of the flow around case C is shown in figure 12. As in case B, two horseshoe vortices have developed.
The snowdrifting calculations in figure 13 shows a higher iso-surface with a larger base area between the cubes than in case B. This is probably because while the amount of snow entering the area is somewhat equal for the two cases, the surface shear stress is lower in case C, caused by of the wider opening between the cubes. This corresponds well with the field measurements.
The upwind snowdrifts also show a variation that corresponds to the measurements in that the most downwind cube have a higher upwind snowdrift. The distances from the cubes to the snowdrifts are 2.0m for the most upwind cube and 1.7m for the neighbouring cube. These distances are measured in the field experiment to be approximately equal to 1.6m for both the cubes. The downwind lateral snowdrifts are also here positioned too far downwind, but the variation in height is reasonably well computed in that the snowdrift near the most downwind cube is higher than the other lateral snowdrift.

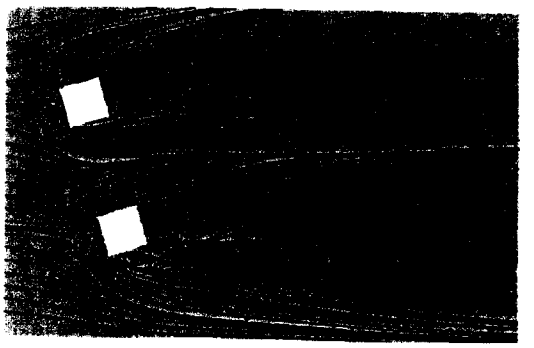

Figure 12. Streamlines around case C.

ensity 1.41 kg/m^3 around

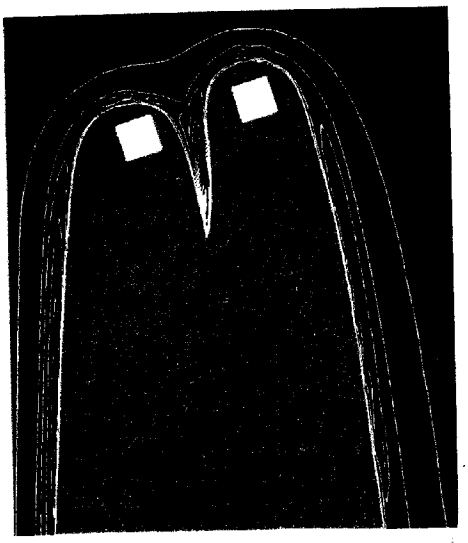

Figure 13. Contoured map of density 1.41 kg/m^3 around case C

4 CONCLUDING DISCUSSION:

The measurements show that the distance between buildings are of vital importance when determining the presence of a centre snowdrift. The funnel effect of the passage between the buildings increases the wind velocity in that area, but since the snowdrifting flux also increases, the carried snow exceeds the carrying capacity of the air, leading to accumulation. When the distance between the buildings is under a certain limit, the horse shoe vortex extends around both buildings. The upwind part of the horse shoe vortex obstructs the transport of snow between the buildings and little snow is entrained in the common wake. In this case, there will be no development of a centre snowdrift. This is also confirmed by the simulations.

The measurements and the numerical simulations show some degree of similarity. The position of the upwind snowdrifts are reasonably well computed, and the presence of a centre snowdrift is possible to interpret from the streamline visualisations. However, the differences between simulations and measurements indicates that the wind pattern and the snow phase concentration around the cubes can be more accurately computed. The reason for the inaccuracies may be the previously mentioned inadequacies in the turbulence model, or that the viscosity of the air/snow mixture satisfy a different relation than the applied one.

The numerical method can be used to determine the best configuration of several building configurations, but is also able to suggest the degree of problems concerning snowdrifts around one specific layout.

REFERENCES

Bang, B., Nielsen, A., Sundsbø, P.A. and Wiik, T. 1994, Computer Simulation of Wind Speed, Wind Pressure and Snow Accumulation around Buildings (SNOW-SIM), *Energy and Buildings*, 21, 235-243.

Beranek, W., J. 1984, Wind environment around single buildings of rectangular shape, *HERON*, 29, no.1.

Chritin, V., Bolognesi, R., Gubler, H. 1998 FlowCapt: A new acoustic sensor to measure snowdrift and wind velocity for avalance forcasting, *Cold Reg. Science and Tech.*, 30, pp.125-133.

Flow Science Inc. 1997, Flow 3D User's Manual, *Flow Science Inc., Los Alamos.*

Haehnel, R. B., Lever, J. H. 1994, Field measurements of Snowdrifts, *Proc. ASCE/ISSW Workshop on Physical Modelling of Wind Transport of Snow and Sand.* Snowbird.

Kawakami, S., Uematsu, T., Kobayashi, T., Kaneda, Y. 1997, Numerical study of a snow wind scoop, *Snow Engineering: Recent advances*, Izumi, Nakamura & Sack (eds), Balkema, Rotterdam. ISBN 90 54108657

Kind, R. J. 1981, Snowdrifting, *Handbook of snow, Principles, Processes, Management and use*, pp. 338-359 Gray, D. M., Male, H. ed.

Thiis, T. K., Gjessing, Y. 1999, Large-Scale measurements of snowdrifts around flat roofed and single pitch roofed buildings, *Cold Reg. Science and Tech.*, 30, pp.175-181.

Thiis, T., K., 2000, A comparison of numerical simulations and full-scale measurements of snowdrifts around buildings, *Wind and Structures*, vol 3.

Tominaga, Y., Mochida, A., 1999 CFD prediction of flow field and snowdrift around a building complex in a snowy region, *J. Wind Eng. and Ind. Aerodynamics*, 81 pp.273-282.

Uematsu, T., Nakata, K., Takeuchi, K., Arisawa, Y., Kaneda, Y. 1991, Three-dimensional numerical simulation of snowdrift, *Cold Reg. Science and Tech.*, 20, pp.65-73.